Research paper

Experimental and modeling study of fluidized bed granulation: Effect of binder flow rate and fluidizing air velocity

U. Vengateson *, Ratan Mohan

Department of Chemical Engineering, Indian Institute of Technology, New Delhi 110016, India

Received 27 June 2016; received in revised form 29 September 2016; accepted 5 October 2016

Available online 10 November 2016

Abstract

Fluidized bed granulation is a widely used technique of producing granules in pharmaceutical, food, detergent, and fertilizer industries. In this study, fluidized bed granulation of two powders – wheat flour and rice powder – with water as binder is studied experimentally and by modeling. The effects of two process parameters – binder flow rate, fluidizing air velocity – are determined. Experimental results show that increasing the binder flow rate favors the formation of bigger granules while increasing fluidizing air velocity leads to a decrease in average granule diameter. Population balance model with suitable form of coalescence kernel (β) has been used to describe the granule growth. Later, this kernel is linked with process parameters – binder flow rate and fluidizing air velocity.

1. Introduction

Granulation is a process of converting small diameter particles into larger diameter agglomerates made up of initial particles. Fluidized bed granulation is one among many methods such as high shear granulation, drum granulation, etc. to produce coarse particles. This method is preferred over other techniques because it provides good mixing, high heat and mass transfer rates, and maintains the bed more or less at uniform temperature [1]. In fluidized bed operation, fine droplets of binder are sprayed on the surface of fluidizing particles. When the wetted particles collide, liquid bridges are formed among particles. The liquid bridges are later converted into solid bridges when they receive sufficient heat from the fluidizing air, to drive off the solvent present. Thus the particles are cemented together to form granule.

Growth of particles in fluidized bed depends on many operating conditions and nature of the feed particle and binder. The particle size range, initially with narrow cut, becomes wider and wider as the granulation process continues and hence particle size distribution (PSD) and average granule diameter changes. These changes are strongly influenced by the process parameters – fluidizing air velocity (FAV), binder flow rate (BFR), bed temperature, bed load, spray characteristics etc., – and physicochemical properties of the binder and feed material. As with all engineering processes, knowledge of the phenomenon and the effect of various parameters are important for the proper design, operation and control of the equipment to get the desired product [2]. Both experimental and modeling/simulation studies on fluidized bed granulation are seen in literature, with an increased interest in the subject in the past twenty years. In general, experimental studies examine the effect of physico-chemical parameters, such as the feed particle characteristics, binder properties (viscosity, surface tension, etc.) and operating variables such as fluidizing air velocity, binder flow rate, inlet air temperature, and bed load, on the product granule size distribution (GSD) and morphology. Modeling studies aim to compute the evolution of the PSD with granulation time, from the initial feed to the final product stage. Most of the models involve population balance approach, in form or another.

In the present work, an experimental and modeling study of fluidized bed granulation of two powders – wheat flour, rice

U. Vengateson is currently working at National Petrochemical Company, Yanbu, Saudi Arabia.

* Corresponding author. Department of Chemical Engineering, Indian Institute of Technology, New Delhi 110016, India. Fax: +966 143252341.

E-mail address: drvengateson@gmail.com; u.vengateson@natpetpp.com (U. Vengateson).

Nomenclature

A	Constant in time dependent β_o, i.e. $\beta_o = At^B$
B	Constant in time dependent β_o, i.e. $\beta_o = At^B$
D_{sv}	Sauter mean diameter, μm
d_i	Average size of particles in ith cut
L_i	Lower limit of particle size in ith bin (μm)
L_{av}	Average particle size in ith bin (μm)
m	Total number of bins
N_i	Number of particles in ith bin
'q_b	Binder flow rate, kg/sec
t_{df}	Granulation time when defluidization starts, min
u_e	Excess gas velocity, m/sec
U_{mf}	Minimum fluidization velocity, m/sec
u	Volume of colliding granule, m^3
u_s	Superficial fluidizing air velocity, m/sec
v_i	Volume of single particle in ith bin, $μm^3$
V_i	Total volume of particles in ith bin, $μm^3$
w_i	Weight of particles staying in ith cut
x_i	Mass fraction of particles in ith cut

Greek letters

β	Coalescence kernel, min^{-1}
β_o	A factor in size dependent coalescence kernel, $\beta = \beta_o(u + v)$
ρ_p	Particle density, kg/m^3

powder – is undertaken. The aim is to experimentally obtain specific granulation data for these powders. These powders were chosen out of interest in fluidized bed granulation of food powders. Wheat flour belongs to more or less Geldart C category whereas rice powder belongs to Geldart A category of powder classification. They are only representative of the food materials and the choice is more from the viewpoint of their being inexpensive and easily available and not for actual use of their granules in food industry. Effect of operating parameters – binder flow rate, fluidizing air velocity – has been studied experimentally in the granulation of the above powders. Modeling of the granulation process has been done using the population balance model with suitably determined form of β. Adjustable constants in β are linked to some of the process parameters.

2. Literature survey

2.1. Binder flow rate (BFR)

The rate at which binder is added to the fluidized bed affects growth rate of particles significantly and it has been studied by many researchers since early 1970s. Davies et al. [3] investigated the effect of binder flow rate (BFR) on the granule characteristics such as avg. diameter, friability, bulk density, and flowability. In their study, 10 kg of powder mix containing lactose and corn starch was granulated using 9.1% aqueous gelatin. The solvent (water) flow rate varied from 85 to

145 g/min till the total quantity of 2200 g of solution was added. The result indicated that increasing binder flow rate caused the formation of bigger granules with more flowability, and decreased bulk density and friability. In the study of Mehta et al. [4] for the granulation of pharmaceutical powder mix – 17.5% sucrose, 69.9% lactose USP, 12.2% starch USP and 0.4% pregelatinized starch – with water as binder, effect of different binder flow rate in the range of 23 ml/min–33 ml/min was investigated. In this study, 500 g of powder mix was granulated with 5 min binder addition, followed by 8 min drying period. It was found that ensuing particle sizes were log-normal and the mean granule diameter was approximately proportional to the liquid flow rate squared and standard deviation was independent of this parameter. Hemati et al. [5] studied the influence of binder flow rate on growth of sand particle. They used two different binders, aqueous NaCl and 1% aqueous CMC solution. When sand was granulated with aqueous NaCl, it was shown that increase in binder flow rate (7.6e-5–16.6e-5 kg/sec) had very little effect on growth rate for a given ratio of NaCl introduced to initial particle mass. On the other hand, for the case of CMC 1%, binder flow rate (145–420 g/hr) had significant effect on growth rate, especially for value greater than 200 g/hr. Boerefijn et al. [6] conducted experiments to study the growth of four particles – hollow glass beads, anhydrous lactose, sodium carbonate, glass ballotini – using PEG 4000 as binder and varied flow rate from 4.8 to 12 kg/hr. It was observed that increase in spray rate increased granule growth for fixed ratio of feed to binder. Tan et al. [7] conducted granulation experiments for glass ballotini – PEG 1500 system – to study the influence of binder flow rate in the range of 3.6 g/min–10 g/min. Though volumetric mean diameter of granules increased with increasing binder flow rate for fixed granulation time, granule size did not significantly change with binder flow rate for a given quantity of binder added to the bed. Jimenez et al. [8] carried out granulation experiments for glass beads and soluble maltodextrin particles agglomerated respectively, with an acacia gum solution and water. They measured both droplet size and liquid jet angle for acacia gum solution. When binder flow rate was increased from 2.65 to 7.75 ml/min, the liquid jet angle increased (33°–40°) as well as the diameter of the liquid droplets (35–45 μm). As a result, the fraction of the bed occupied by the wetting – active zone – increased from 14% to 29% and the penetration depth of the liquid jet increased from 14 to 17 cm [9]. α-lactose monohydrate was granulated in miniaturized fluidized bed by spraying polyvinylpyrrolidone of different concentrations (6%, 8%, 10% w/w) using electrostatic nozzle. D10, D50, and D90 of granules after 3 min of operation for different binder flow rates (16–18, 30–36, 48, 66–68, 94–96 g/hr) were reported in 3D plot and growth was observed significant when flow rate exceeds 36 g/hr. Different methods of binder addition, wet and dry, were studied to produce pharmaceutical granule of size 150–300 μm by Osborne et al. [10]. Granola breakfast cereal was produced in fluidized bed granulation by Pathare et al. [11] and the effect of binder flow rate on granule size was studied. By spraying aqueous solution of ammonium sulfate on core particles of size 0.9–1.6 mm, large spherical granules were produced by Wang et al. [12] and also

the effect of adding $CaCO_3$ and SiO_2 particles into feed solution on coating efficiency was investigated. Recently, Rieck et al. [13] studied the effect of spray rate on particle size distribution. They sprayed sodium benzoate solution on the porous ($\gamma - Al_2O_3$) and nonporous (glass) initial particles.

2.2. Fluidizing air velocity (FAV)

Fluidizing air velocity is one of the important parameters which determine granule growth rate and characteristics since it affects particle mixing, binder dispersion, drying rate and operation stability. Smith and Nienow [14] carried out experiments to study the growth of glass powder by using two different binders – 10% benzoic acid solution in methanol (weak binder) and 5% Carbowax in methanol (strong binder). Investigations were made for different excess gas velocities, ranging from 15 cm/sec to 65 cm/sec. Two different growth mechanisms were observed – at low gas velocities, particle growth is due to agglomeration but at high gas velocities, layering becomes dominant and growth depends only on quantity of material deposited, independent of excess gas velocity. Hemati et al. [5] studied the effect of fluidizing air velocity on agglomeration of sand particles using 1% CMC solution. They conducted experiments for three different excess gas velocities and also observed growth rate to decrease as excess velocity increases. They also found that the granules formed at low excess velocities were less friable. Tan et al. [7] investigated the influence of fluidizing air velocity on growth of glass ballotini using PEG 1500 and found that initial growth rate was faster for lower fluidizing air velocity (U = 0.83 m/sec, U/U_{mf} =16.6), but later growth proceeded at a rate similar to that at higher velocity. They have also shown that the granule size distribution became narrower with increased fluidization. In a variation of the usual fluidized bed, Tsutsumi et al. [15] recommended the use of fast fluidized bed for homogeneous agglomeration due to its potential to produce granules with narrow size distribution. Charinpanitkul et al. [16] studied the effect of fluidizing air velocity – 0.8, 1, 1.2 m/sec – on growth of two different formulations. In first formulation, 500 g of lactose was used in bed and in the second formulation, 350 g lactose and 150 g corn starch were used. In both formulations, 2.5 g of Cab-O-Sil (colloidal silicon dioxide) was added in the bed materials as an anti-cohesive material. Binder solution of 5% (w/w) PVP type K30 was used for both cases. Mode of binder addition is not continuous but 10 sec spraying and then 20 sec no-spraying. In this way, operation was continued till 100 ml was added. Their results showed that an increase in fluidizing air velocity caused increasing amount of fine particles, leading to the smaller average particle size [17]. Growth of acerola powder for different fluidizing air velocity (1.44 Umf–6.33 Umf) with different inlet air temperatures was aimed at identifying optimum process conditions for maximum granule size for given yield. In addition to fluidizing air velocity (superficial velocity), the ratio of the superficial velocity to minimum fluidization velocity (U_s/U_{mf}) is also an important parameter as it affects the bed expansion and resulting solid concentration in a manner given by Richardson and Zaki [18] equation. Boerefijn and Hounslow [6], in their study on growth of different types of particles

(hollow glass beads, anhydrous lactose, sodium carbonate, glass ballotini), fixed this ratio at a value of approximately 23 so that similar solid concentration in the spray zone could be maintained for the entire above particle systems. Recently, Moraga et al. [19] studied the effect of different parameters including fluidizing air velocity of the growth of seed particles with the binder of identical melt nature.

3. Materials and methods

The powders – wheat flour, rice powder – were procured in bulk. The actual feed was prepared by sieving the powders through a 150 μm screen. The undersize fraction was mixed well and used for feed. Feed characterization and the minimum fluidization velocity are shown in Table 1.

The experimental set up used in this study is shown in Fig. 1. It consists of a cylindrical column of 6.35 cm diameter and 20 cm height and with a conical upper section of height 20 cm and top diameter 12.7 cm. The column is closed by a lid containing six bag filters to prevent particle elutriation. The air required for fluidization is supplied by a blower and is passed through a heater. Before entering the bed, its flow rate, humidity and temperature are measured. To spray the binder, a nozzle is inserted vertically inside the column and its tip is located about 10 cm from the distributor so that the spray is fully submerged when the particles are fluidized. The binder (in the present case water) is drawn by a peristaltic pump into the nozzle where it is atomized by a compressed air jet. The compressed air or 'atomizing air' flow rate is also measured. Two thermocouples, one beneath the distributor plate and another in the bed, are inserted to measure the inlet air temperature and bed temperature respectively.

A known quantity of powder is taken in the bed. Initial moisture present in the powder, if any, can be removed in the fluidized bed itself by passing hot air. Twin phase nozzle is inserted into the fluidized bed at chosen height. Air is allowed to enter the bed at the required superficial air velocity to fluidize the powder. Peristaltic pump is switched on to the preset flow rate of binder. This time, it is the start of the granulation process, i.e. t = 0. Granulation is allowed to occur up to a maximum possible operating time, i.e. defluidization time, t_{df}. Immediately, both peristaltic pump and blower are switched off to stop binder addition and fluidization respectively. The column is emptied and the whole mass is dried and stored for size distribution analysis. During the process of granulation, bed temperature and pressure drop are also recorded.

Granules produced are sieved into many fractions. Hand sieving is preferred as it is gentler and reduces attrition. The

Table 1
Feed particle characterization.

Property	Wheat flour	Rice powder
Average particle size, D_{sv} (μm)	38	52
True density (kg/m³)	1450	1570
Bulk density (kg/m³)	545	816
u_{mf} (cm/sec) [20]	0.07	0.13
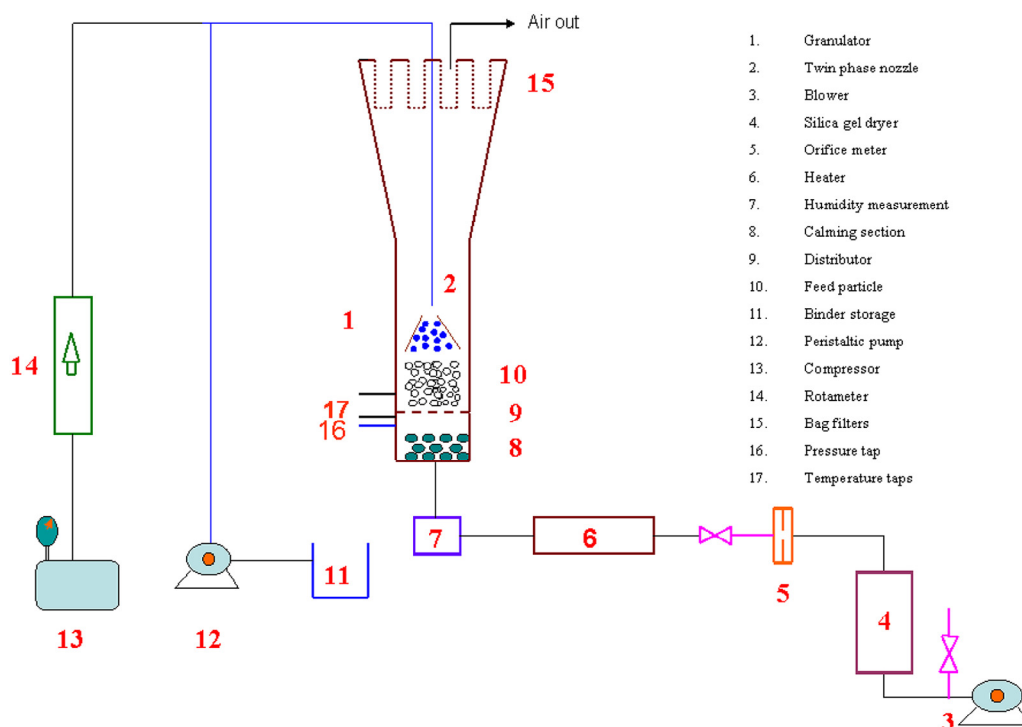
Fig. 1. Fluidized bed granulator: Experimental set up.

1.	Granulator
2.	Twin phase nozzle
3.	Blower
4.	Silica gel dryer
5.	Orifice meter
6.	Heater
7.	Humidity measurement
8.	Calming section
9.	Distributor
10.	Feed particle
11.	Binder storage
12.	Peristaltic pump
13.	Compressor
14.	Rotameter
15.	Bag filters
16.	Pressure tap
17.	Temperature taps

material that stayed in each size range is weighed. Average size (Sauter mean diameter) is determined by Eq. (1).

$$D_{sv} = \frac{1}{\sum \frac{x_i}{d_i}} \qquad (1)$$

where x_i, d_i represent mass fraction and arithmetic average size of the particles in 'i' cut.

The maximum possible operating time is defluidization time, t_{df}, however, it is not at all desired in industry due to formation of more clumps. In practice, granulation is stopped at 65–85% of defluidization time, depending on feed and binder characteristics. Due to non availability of on-line size distribution measurement facility and the fact that ultimately sieving would be used for analysis, it was not considered feasible to interrupt the granulation runs at intermediate times to measure the granule size distribution (GSD). The difficulty was overcome by taking as many feed batches (from the same initial well mixed feed powder) as the times at which PSD measurements are to be made. Then each batch was granulated for its designated time, e.g. one batch for 4 minutes, another for 6 minutes, etc.

4. Results and discussion

According to Geldart classification of particles [21] the particles – wheat flour, rice powder – fall in the category of Group A. However, wheat flour behavior during fluidization is like Group C category. It may be due to its inherent nature of stickiness. When wheat flour was fluidized, initially there was channeling and parts of particles rose as a plug of solids,

disintegrated, and then vigorous agitation occurred. Rice powder expanded considerably during fluidization before bubbles appear and gross circulation of particles occurred. As stated earlier, growth of particles in fluidized bed depends on various parameters. In this section, the effect of parameters – binder flow rate, fluidizing air velocity – is discussed below.

4.1. Effect of binder flow rate (BFR)

Fig. 2 shows the effect of binder flow rate on the granule growth of wheat flour by means of an average diameter (D_{sv}) vs time plot. It is seen from the figure that increasing the binder flow rate from 2 ml/min to 4 ml/min causes the formation of bigger granules at a quicker rate. It is due to the fact that increasing the binder flow rate results in more binder availability in spraying zone and hence more wetting and sticking of the particles. However, high growth rate also results in earlier defluidization. For example, when binder is added at 3 ml/min, experiment had to be stopped at 5 min due to defluidization. Similar experimental results for the growth of rice powder are shown in Fig. 3.

4.2. Effect of fluidizing air velocity (FAV)

To examine the effect of fluidizing air velocity, two velocity values were used. This selection of velocities is based on consideration of particle elutriation and adjustment of air flow rate so that particles are fluidized. Fig. 4 shows the effect of fluidizing air velocity on the growth of wheat flour. The results show that increasing fluidizing air velocity caused the formation of smaller size granules and the defluidization was delayed. Probable reason is that higher fluidizing air velocity increases the relative collisional velocity between the particles and hence the
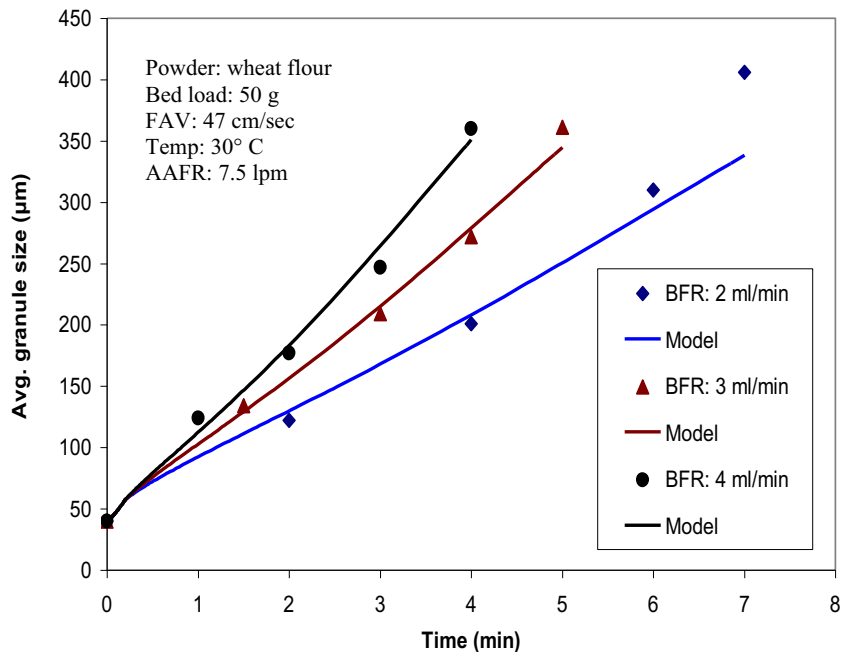
Fig. 2. Effect of BFR on growth of wheat flour (R1, R2, R3).

probability of coalescence of particles during collision is reduced. Further, the higher collisional velocity will also cause more attrition and hence reduction in granule size [22]. Another possible reason is that some of the fine droplets of binder may be swept away from the bed before they are able to impinge on the particles when it is operated at high fluidizing air velocity. Higher flow air caused faster powder circulation and increases the powder flux through the spray zone, which will subsequently lead to improved binder addition and reduced chances of bed quenching. Fig. 5 shows the effect of fluidizing air velocity on the growth of rice powder. The onset of defluidization occurred at 4 min for fluidizing air velocity at 27 cm/sec whereas it was delayed 6.5 min for the case of 47 cm/sec.

4.3. Modeling

The evolution of particle size distribution during granulation (agglomeration) is simulated using the discretized population equation of Hounslow et al. [23], given by Eq. (2).
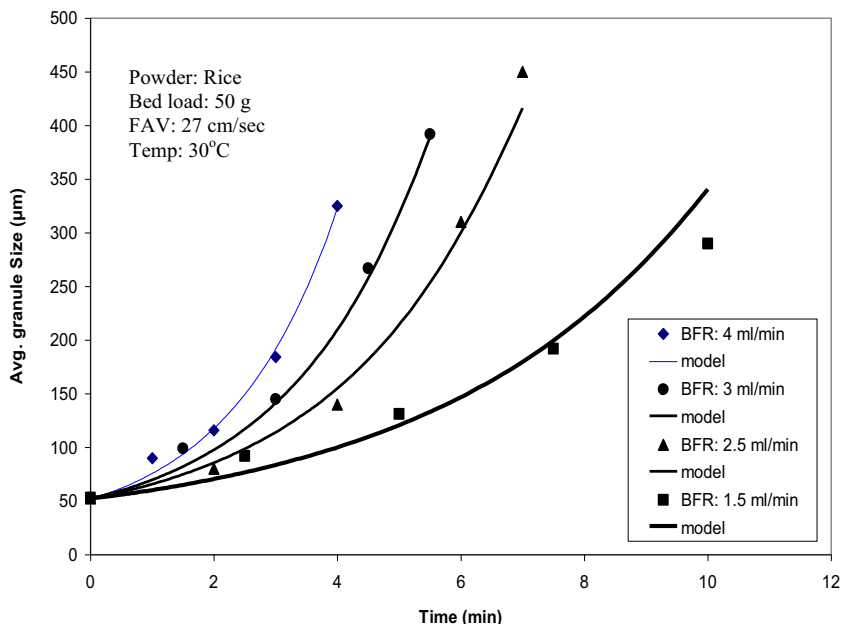

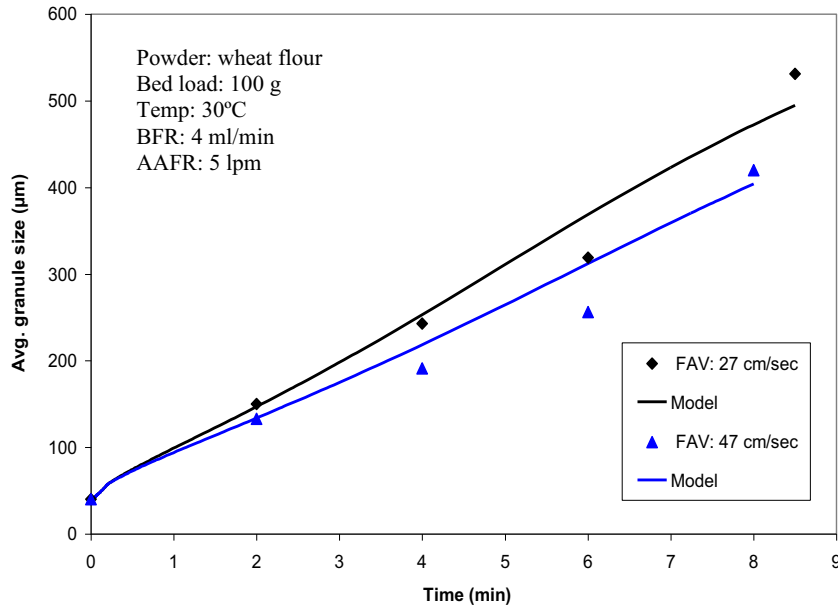Fig. 3. Effect of BFR on growth of rice powder (R1, R2, R3, R4).

Fig. 4. Effect of FAV on growth of wheat flour (R4, R5).

$$\frac{dN_i}{dt} = N_{i-1} \sum_{j=1}^{i-2} 2^{j-i+1} \beta_{i-1,j} N_j + \frac{1}{2} \beta_{i-1,i-1} N_{i-1}^2 - N_i \sum_{j=1}^{i-1} 2^{j-i} \beta_{i,j} N_j$$

$$- N_i \sum_{j=i}^{\infty} \beta_{i,j} N_j \qquad (2)$$

In this model, particle size spectrum is divided into 'm' bins such that particle volume ratio of upper and lower limits of the 'i'th interval is two ($v_{i+1} = 2v_i$). This model is based on binary interaction of particles belonging to two bins.

The particle size range is assumed to span from the lowest particle size in feed to the expected maximum granule size. Then, the size range is divided into 'm' number of bins so that $L_{i+1} / L_i = 2^{1/3}$. The number of particles in each bin (N_i), where 'i' ranges from 1 to m for any time 't', is obtained by solving the above set of differential equations by Runge–Kutta 4th order method. There should always be an empty interval at the end of the particle size distribution to avoid finite domain error. The finite domain error can be monitored by checking the total mass of granules which has to be conserved during computations.
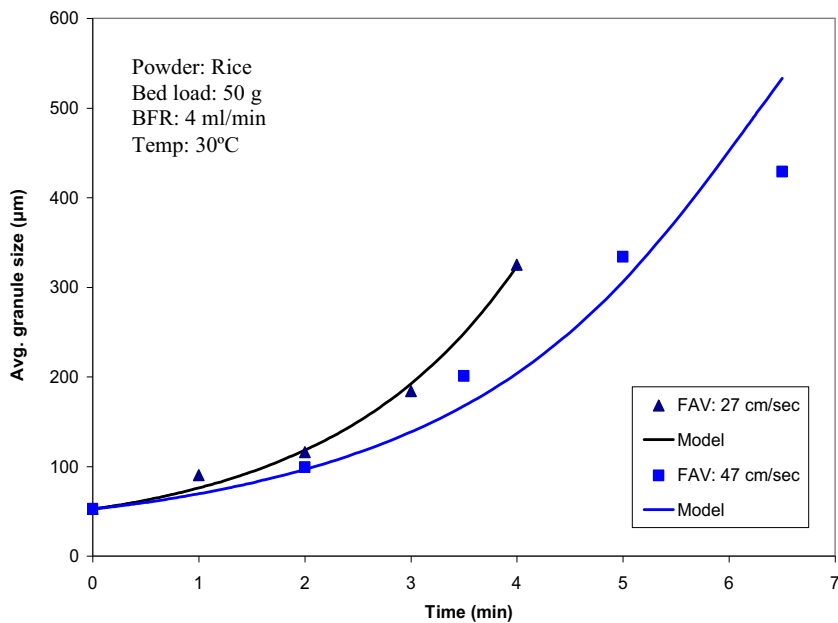

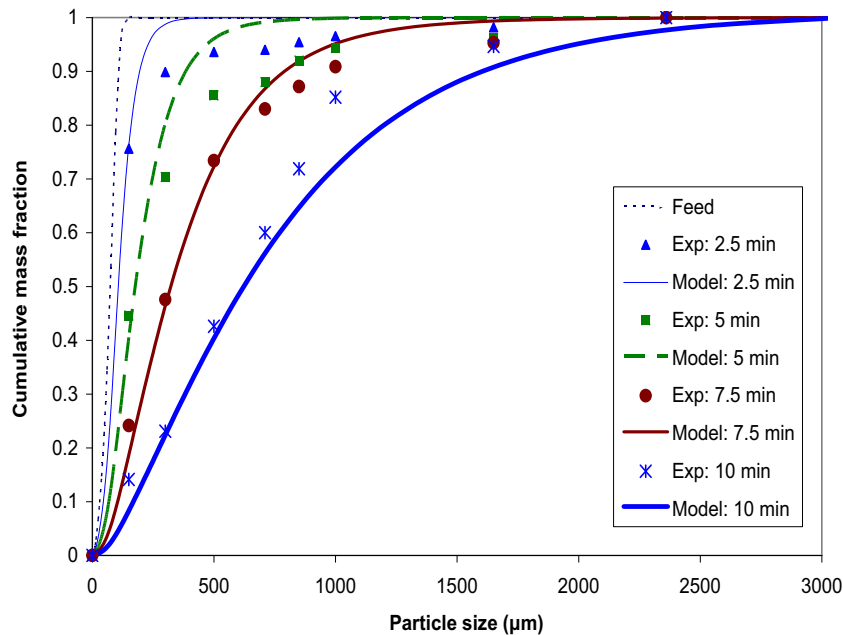Fig. 5. Effect of FAV on rice granule growth (R4, R5).

Fig. 6. Rice powder: Comparison of experimental GSD with model GSD for R1.

It may be seen that the ability of Eq. (2) to simulate a complicated granulation process depends very much on what the β_{ij} (the coalescence kernel) is; since all the physics of the process gets lumped into there. However, assuming that suitable β_{ij} is known, the solution of the differential equations begins with the initial condition. The initial condition is obtained from the feed size distribution curve. Either directly the number feed distribution may be available or, as is more often the case, the measured volume/mass distribution is converted to the number of particles in ith bin (N_i) by Eq. (3).

$$N_i = \frac{w_i}{\rho_p v_i} = \frac{V_i}{v_i} \qquad (3)$$

Particle density is assumed unchanged during simulation, however, in experiments granules hold binder and the density of granule may be different from that of feed particles. Once all the bins in the feed are filled by corresponding numbers, remaining bins out of 'm' bins are assigned value '0', i.e. they are taken empty. Eq. (2) is then integrated numerically with a suitable time step Δt and the number distributions at subsequent times are obtained. These may then be converted to any desired form such as cumulative mass distribution vs time or D_{sv} vs time. Dsv is calculated from Eq. (4).

$$D_{sv} = \frac{\sum N_i L_{av}^3}{\sum N_i L_{av}^2} \qquad (4)$$

To match the simulation results with experimental observations, some of the various forms of β available in literature [24] were tested. Linear form of coalescence kernel, $\beta = \beta_0(u + v)$, appears to be the best choice and with this kernel, simulation results are obtained and compared to experimental data. Though growth patterns are similar, degree of concavity of

simulation results (D_{sv} vs t) with constant β_0 in linear model is different from that of experimental growth, i.e. experimental D_{sv} vs t. To get a better agreement, β_0 is taken as a function of time ($\beta_0 = A*t^B$) with two adjustable parameters A and B. With this time dependent β_0, simulation results for the granule size distribution (GSD) are compared with the experimental GSD.

The values of A and B are obtained by minimizing the errors between the values of simulation D_{sv} and the experimental D_{sv}. For rice powder, initially both 'A' and 'B' are found but subsequently 'B' was fixed to B = 0.1 and only 'A' value was regressed from the data and these values are shown for each experimental run in Table 2. Comparison of experimental D_{sv} and the model D_{sv} for all the runs is shown in Figs. 3 and 5. Further, the cumulative size distributions are shown in Figs. 6–10. Similar to rice powder, agglomeration rate constant (kernel) is obtained from the experimental D_{sv} data for wheat flour granulation. However the growth of wheat flour is different and in this case it was required to keep the coalescence kernel constant in the beginning – primary growth, and then take it size dependent — secondary growth, as shown in Eq. (6). The agglomeration rate constant in the secondary growth, β_0 is again taken to be a function of time with two parameters as

Table 2
Details of parameters for rice powder experimental runs.

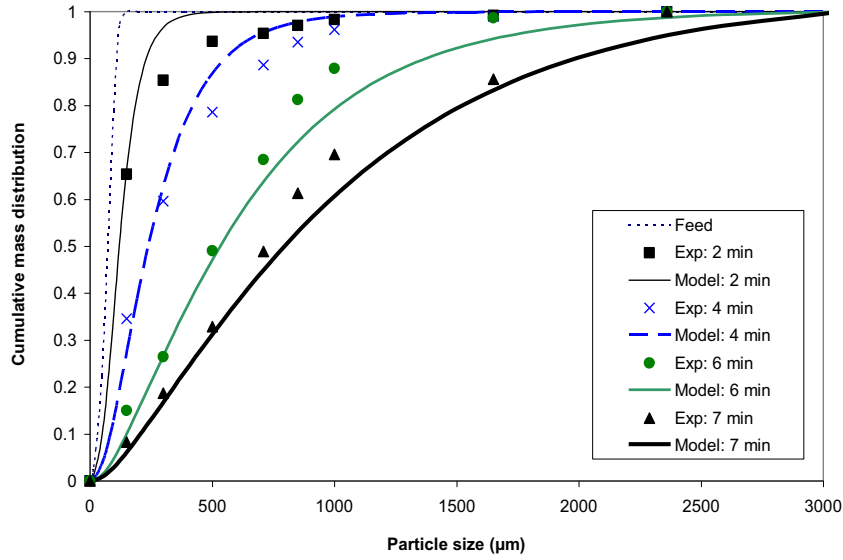| Run No.	Binder flow rate (ml/min)	Fluidizing air velocity (cm/sec)	Inlet air temperature (°C)	Bed load (gm)	Atomizing air flow rate (lpm)	Model parameter A
R1	1.5	27	30	50	5	8.9E-15
R2	2.5	27	30	50	5	15E-15
R3	3	27	30	50	5	19E-15
R4	4	27	30	50	5	25E-15
R5	4	47	30	50	5	18E-15

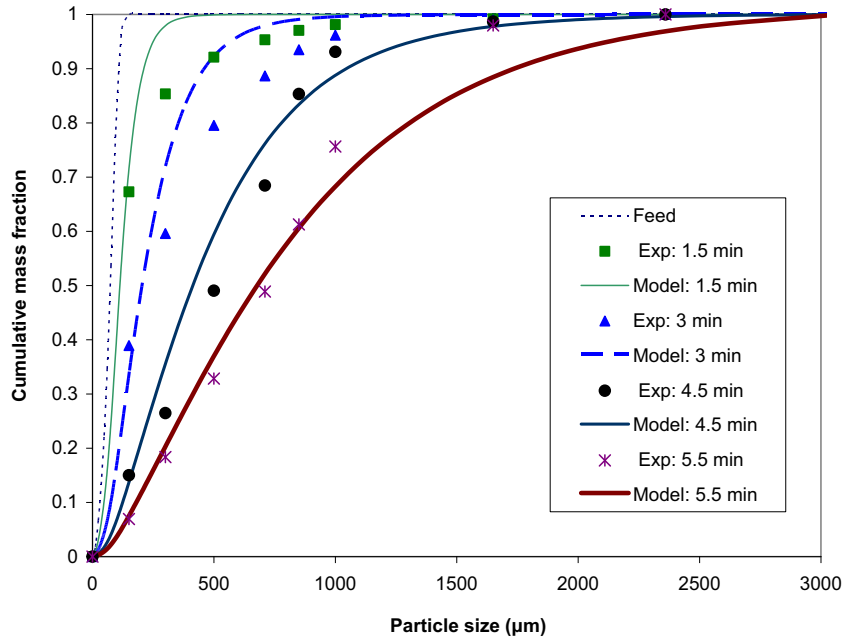Fig. 7. Rice powder: Comparison of experimental GSD with model GSD for R2.

Fig. 8. Rice powder: Comparison of experimental GSD with model GSD for R3.

$\beta_0 = A*t^B$, and these constants are obtained as described earlier. This time the value of model parameter 'B' is fixed for all simulations as $B = -0.6$ and 'A' values for each experimental run are determined and shown in Table 3. Comparison of experimental D_{sv} and the model D_{sv} for all the runs is shown in Figs. 2 and 4. Further, the cumulative size distributions are shown in Figs. 11–15. Dsv vs t prediction results are good for rice powder, except for a few cases. For the wheat flour case, deviations are seen for intermediate D_{sv} values too. Wheat flour experimental D_{sv} vs t shows a slight convexity initially and although it has been tried to take care of this by taking constant β for t < 0.2, either the choice of the cut off time is not correct or the parameter A is not of right value.

Table 3
Details of parameters of wheat flour experimental runs.

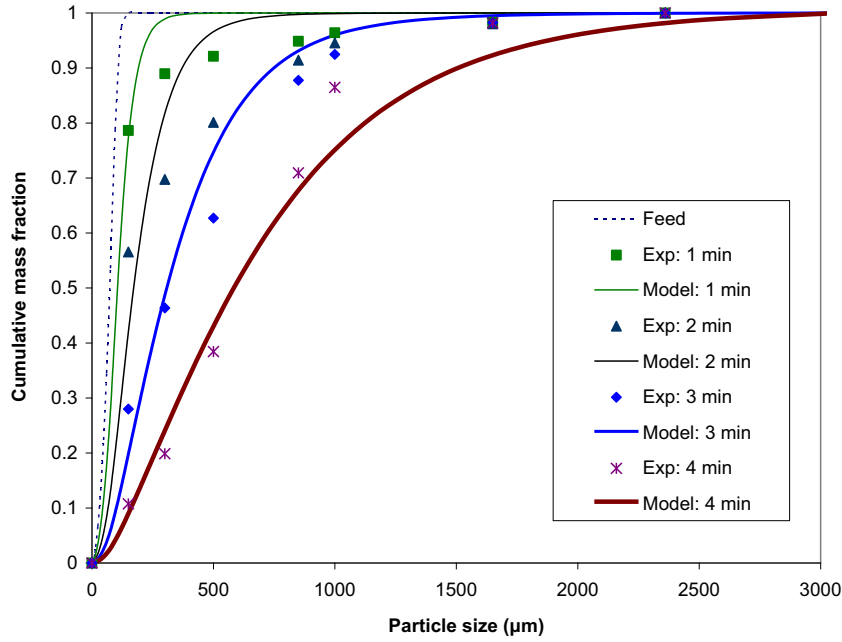| Run No.	Binder flow rate (ml/min)	Bed load (gm)	Inlet air temperature (°C)	Fluidizing air velocity (cm/sec)	Atomizing air flow rate (lpm)	Model parameter A
R1	2	50	30	47	7.5	23.5E-15
R2	3	50	30	47	7.5	27.5-15
R3	4	50	30	47	7.5	31E-15
R4	4	100	30	27	5	26E-15
R5	4	100	30	47	5	22E-15

Fig. 9. Rice powder: Comparison of experimental GSD with model GSD for R4.

4.4. Relation of β with process variables

The different forms of β used for granulation of rice powder and wheat flour are given below (Eqs. 5 and 6).

Rice powder:

$$\beta = \beta_o (u + v), \quad \beta_o = At^B \quad B = 0.1 \tag{5}$$

Wheat flour:

$$\beta = \begin{cases} \beta_0 = 15e\text{-}9 & t < 0.2 \\ \beta_0 (u+v), \beta_0 = At^B & t > 0.2 \end{cases} \quad B = -0.6 \tag{6}$$

β_o used for above powders in Eqs. (5) and (6) is a time dependent function with two parameters, A and B. The parameter B is fixed as a constant for each powder while parameter A varies with process conditions as shown in Tables 2 and 3. Biggs et al. [25] also used time dependent β to describe the breakage during spray off period in fluidized bed granulation. Although several process variables affect the granule growth and hence A, an attempt has been made to correlate A with some process parameters through a factor $\left[\dfrac{q_b}{\rho_p u_s} \right]$. The factor was used by Boerefijn and Hounslow [6] as a scaling parameter
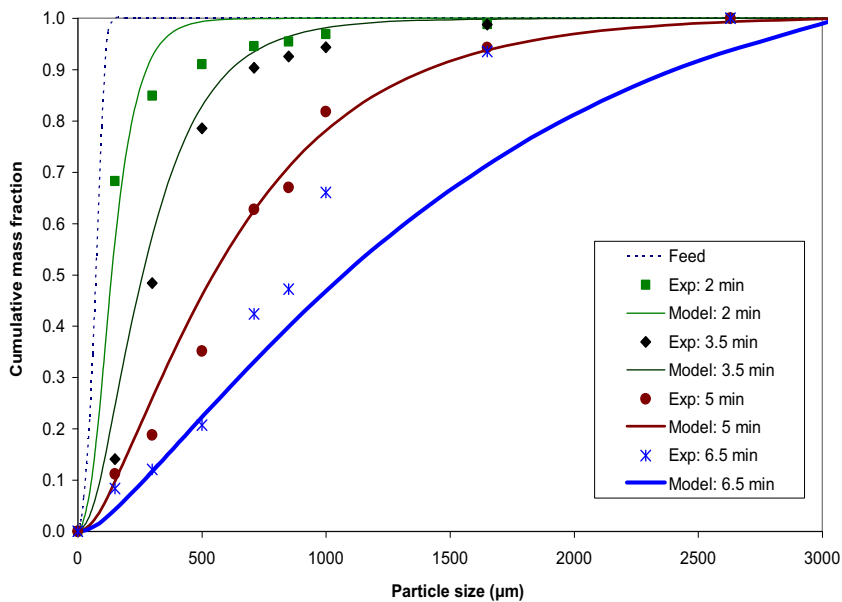

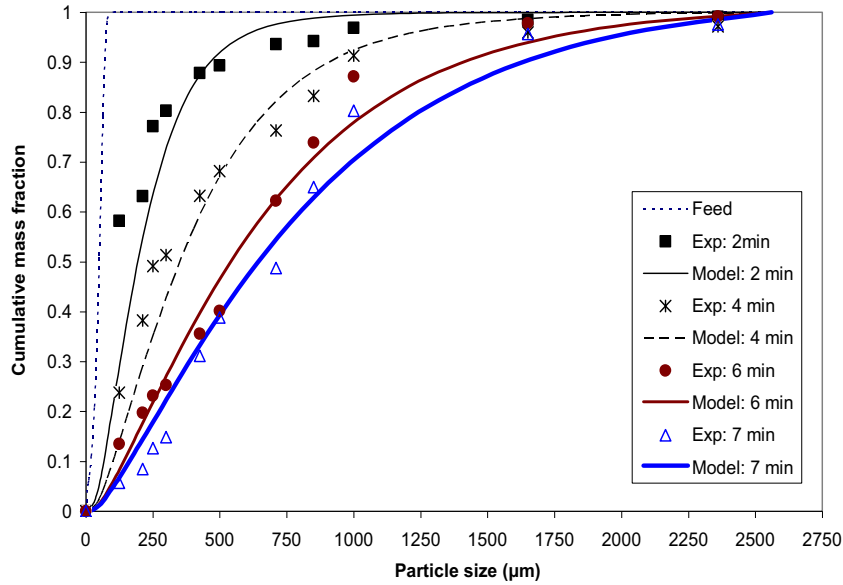Fig. 10. Rice powder: Comparison of experimental GSD with model GSD for R5.

Fig. 11. Wheat flour: Comparison of experimental GSD with model GSD for R1.

to scale up the granulation process based on similarity of contacting conditions (A_{spray}) and fluidization conditions (u_e). But in this work, it is used only to correlate with coalescence kernel. This scaling factor is practically the same as functional group in Akkermans or flux number, $\log_{10}\left(\dfrac{\rho_p u_e}{q_b A_{spray}}\right)$. The excess gas velocity ($u_e = u_s - u_{mf}$) in flux number is considered the same as u_s in scaling factor since $u_{mf} << u_s$.

Eq. (7) and Eq. (8) are made to correlate A with scaling factor for rice powder and wheat flour respectively, by considering only the relevant runs.

$$A = 2 \times 10^{-7} \left[\frac{q_b}{\rho_p u_s}\right] + 1 \times 10^{-15} \tag{7}$$

$$A = 2 \times 10^{-7} \left[\frac{q_b}{\rho_p u_s}\right] + 2 \times 10^{-14} \tag{8}$$

The disadvantage of above approach is some parameters, for example inlet air temperature and viscosity, are not included. Another approach which connects β with process parameters is through Stokes number [26,27], which also lacks some process parameters. A rigorous method should link β with all
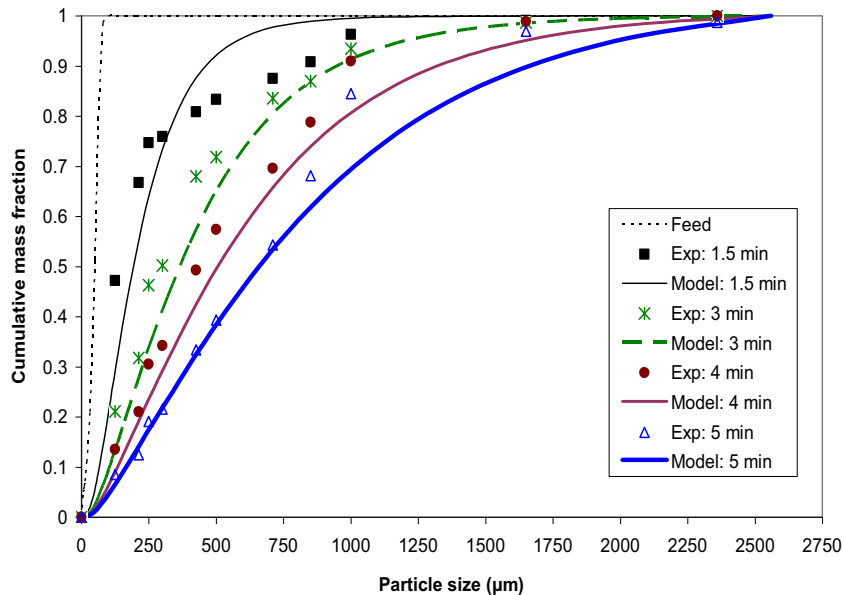

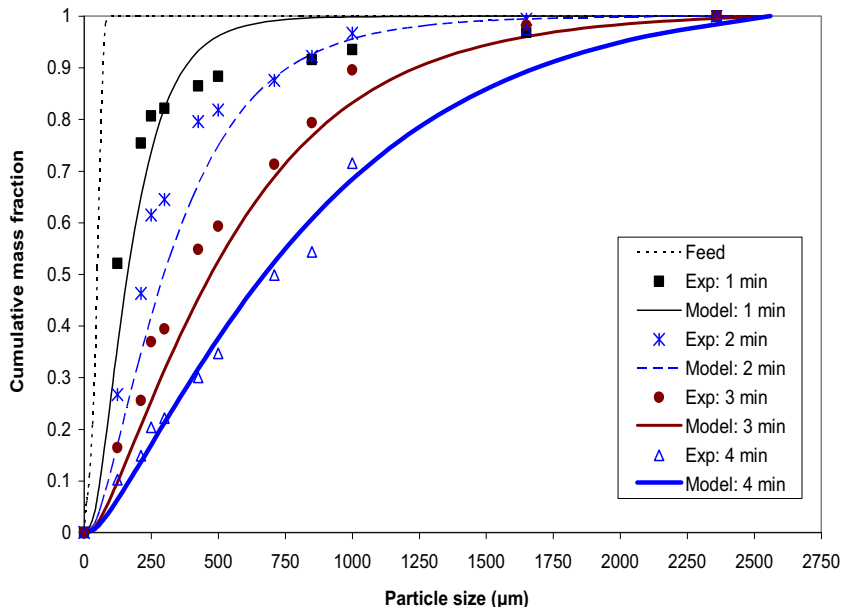Fig. 12. Wheat flour: Comparison of experimental GSD with model GSD for R2.

Fig. 13. Wheat flour: Comparison of experimental GSD with model GSD for R3.

the important process variables and physico-chemical properties of the feed and binder, but as of now no such complete model is available.

5. Conclusion

Effect of process parameters – binder flow rate, fluidizing air velocity – on growth of two food powders – wheat flour, rice powder – has been studied experimentally and by simulation. Granule growth rate and the size of the end granules increase with the binder flow rate, however, increased binder flow rate causes earlier defluidization. Increase in fluidizing air velocity led to a reduction in growth rate and delayed defluidization. Discretized population equation was used to describe the

granule growth. The equation describes the granule growth kinetics in terms of the coalescence kernel β. A size dependent kernel $\beta = \beta_o(t)*(u + v)$ where $\beta_o(t) = At^B$ (i.e. two parameter time dependent function) was used for rice powder. For wheat flour, same linear model but $\beta_o(t) = (\beta_o + At^B)$ was used to account primary growth. 'A' and 'B' were obtained from experimental data. Parameter 'A' and hence ($\beta_o = At^B$) did show some trend in variation with process parameters. 'A' was therefore correlated with binder flow rate and fluidizing air velocity through a factor $\left[\dfrac{q_b}{\rho_p u_s}\right]$ in flux number and it was found to be a linearly increasing function of this factor. With the correlated β_o, it is possible to predict growth rate for new set of conditions,
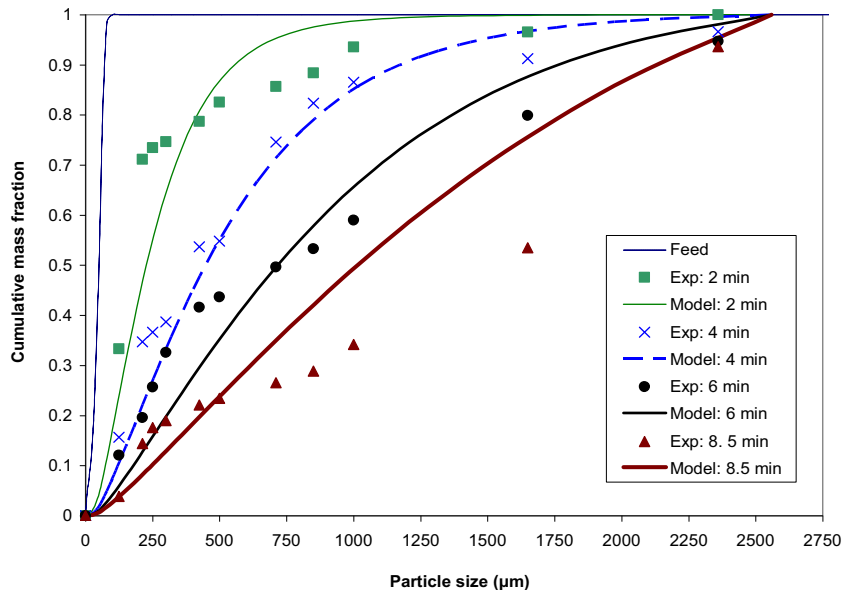

Fig. 14. Wheat flour: Comparison of experimental GSD with model GSD for R4.
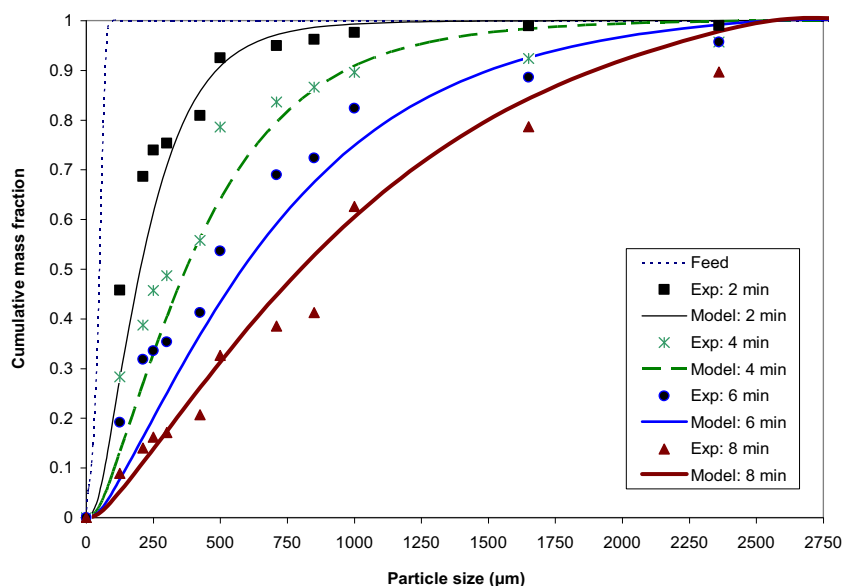
Fig. 15. Wheat flour: Comparison of experimental GSD with model GSD for R5.

though limited to variables q_b and u_s and in the range of values similar to that in this study.

References

[1] O. Planinšek, R. Pišek, A. Trojak, S. Srčič, The utilization of surface free-energy parameters for the selection of a suitable binder in fluidized bed granulation, Int. J. Pharm. 207 (1) (2000) 77–88.

[2] M. Ganesapillai, P. Simha, The rationale for alternative fertilization: equilibrium isotherm, kinetics and mass transfer analysis for urea-nitrogen adsorption from cow urine, Resour. Effic. Technol. 1 (2) (2015) 90–97.

[3] W.L. Davies, W.T. Gloor, Batch production of pharmaceutical granulations in a fluidized bed 1: effect of process variables on physical properties of final granulation, J. Pharm. Sci. 60 (12) (1971) 1869–1874.

[4] A. Mehta, K. Adams, M.A. Zoglio, J.T. Carstensen, Influence of granulation liquid flow rate on particle size distribution in spray granulated products, J. Pharm. Sci. 66 (10) (1977) 1462–1464.

[5] M. Hemati, R. Cherif, K. Saleh, V. Pont, Fluidized bed coating and granulation: influence of process related variables and physicochemical properties on the growth kinetics, Powder Technol. 130 (2003) 18–34.

[6] R. Boerefijn, M.J. Hounslow, Studies of fluid bed granulation in an industrial R&D context, Chem. Eng. Sci. 60 (2005) 3879–3890.

[7] H.S. Tan, A.D. Salman, M.J. Hounslow, Kinetics of fluidized bed melt granulation – 1: the effect of process variables, Chem. Eng. Sci. 61 (2006) 1585–1601.

[8] T. Jimenez, C. Turchiuli, E. Dumoulin, Particles agglomeration in a conical fluidized bed in relation with air temperature profiles, Chem. Eng. Sci. 61 (2006) 5654–5661.

[9] N. Kivikero, M. Murtomaa, B. Ingelbeen, O. Antikainen, E. Rasanen, J.P. Mannermaa, et al., Microscale granulation in a fluid bed powder processor using electrostatic atomisation, Eur. J. Pharm. Biopharm. 71 (2009) 130–137.

[10] J.D. Osborne, R.P. Sochon, J.J. Cartwright, D.G. Doughty, M.J. Houslow, A.D. Salman, Binder addition methods and binder distribution in high shear and fluidized bed granulation, Chem. Eng. Res. Des. 89 (5) (2011) 553–559.

[11] P.B. Pathare, N. Bas, J.J. Fitzpatrick, K. Cronin, E.P. Byrne, Production of granola breakfast cereal by fluidized bed granulation, Food Bioprod. Process. 90 (3) (2012) 549–554.

[12] G. Wang, L. Yang, R. Lan, T. Wang, Y. Jin, Granulation by spray coating aqueous solution of ammonium sulfate to produce large spherical granules in a fluidized bed, Particuology 11 (2013) 483–489.

[13] C. Rieck, T. Hoffmann, A. Buck, M. Peglow, E. Tsotsas, Influence of drying conditions on layer porosity in fluidized bed spray granulation, Powder Technol. 272 (2015) 120–131.

[14] P.G. Smith, A.W. Nienow, Particle growth mechanisms in fluidized bed granulation - 1, Chem. Eng. Sci. 38 (8) (1983) 1223–1231.

[15] A. Tsutsumi, H. Suziki, Y. Saito, K. Yoshida, R. Yamazaki, Multi component granulation in a fast fluidized bed, Powder Technol. 100 (1998) 237–241.

[16] T. Charinpanitkul, W. Tanthapanichakoon, P. Kulvanich, K.S. Kim, Granulation and tabletization of pharmaceutical lactose granules prepared by a top-sprayed fluidized bed granulator, J. Ind. Eng. Chem. 14 (2008) 661–666.

[17] G.C. Dacanal, F.C. Menegalli, Experimental study and optimization of the agglomeration of acerola powder in a conical fluid bed, Powder Technol. 188 (2009) 187–194.

[18] J.F. Richardson, W.N. Zaki, Sedimentation and fluidization: part 1, T. I. Chem. Eng. 32 (1954) 35–53.

[19] S.V. Moraga, M.P. Villa, D.E. Bertin, I.V. Cotabarren, J. Pina, J. Pina, et al., Fluidized bed melt granulation: the effect of operating variables on process performance and granule properties, Powder Technol. 286 (2015) 654–667.

[20] C.Y. Wen, Y.H. Yu, A generalised method for predicting the minimum fluidization velocity, AIChE J. 12 (1966) 610–612.

[21] D. Geldart, Types of gas fluidization, Powder Technol. 7 (1973) 285–292.

[22] M. Ganesapillai, P. Simha, K. Desai, Y. Sharma, T. Ahmed, Simultaneous resource recovery and ammonia volatilization minimization in animal husbandry and agriculture, Resour. Effic. Technol. 2 (1) (2016) 1–10.

[23] M.J. Hounslow, R.L. Ryall, V.R. Marshall, A discretized population balance for nucleation, growth, and agglomeration, AIChE J. 34 (11) (1988) 1821–1832.

[24] I.T. Cameron, F.Y. Wang, C.D. Immanule, F. Stepanek, Process systems modeling and applications in granulation: a review, Chem. Eng. Sci. 60 (2005) 3723–3750.

[25] C. Biggs, R. Boerefijn, M. Buscan, A. Salman, M. Hounslow, Fluidized bed granulation: modelling the growth and breakage kinetics using population balances, Paper No. 226, 4th World Congress on Particle Technology, Sydney, Australia, 2002.

[26] S.A. Cryer, Modeling agglomeration processes in fluid bed granulation, AIChE J. 45 (10) (1999) 2069–2078.

[27] S.A. Cryer, P.N. Scherer, Observations and process parameter sensitivities in fluid bed granulation, AIChE J. 49 (11) (2003) 2802–2809.